

9-13-2005

Interactions of Fano resonances in the transmission of an Aharonov-Bohm ring with two embedded quantum dots in the presence of a magnetic field

Yong S. Joe
Ball State University

Arkady M. Satanin
Ball State University

Gerhard Klimeck
gekco@purdue.edu

Follow this and additional works at: <http://docs.lib.purdue.edu/nanodocs>

Joe, Yong S.; Satanin, Arkady M.; and Klimeck, Gerhard, "Interactions of Fano resonances in the transmission of an Aharonov-Bohm ring with two embedded quantum dots in the presence of a magnetic field" (2005). *Other Nanotechnology Publications*. Paper 120. <http://docs.lib.purdue.edu/nanodocs/120>

This document has been made available through Purdue e-Pubs, a service of the Purdue University Libraries. Please contact epubs@purdue.edu for additional information.

Interactions of Fano resonances in the transmission of an Aharonov-Bohm ring with two embedded quantum dots in the presence of a magnetic field

Yong S. Joe,¹ Arkady M. Satanin,^{1,2} and Gerhard Klimeck³

¹Center for Computational Nanoscience, Department of Physics and Astronomy, Ball State University, Muncie, Indiana 47306, USA

²Institute for Physics of Microstructures, RAS, GSP-105, Nizhny Novgorod, 603950 Russia

³Network for Computational Nanotechnology, School of Electrical and Computer Engineering, Purdue University, West Lafayette, Indiana 47907, USA

(Received 23 June 2005; published 13 September 2005)

Interactions of Fano resonances in the transmission for an Aharonov-Bohm ring with two embedded quantum dots are examined. As the interaction parameter between two quantum dots is modulated, two Fano dipoles (a resonance zero-pole pair) in the complex-energy plane form a quasiparticle, which behaves as a coupled object called a “*Fano quadrupole*.” In the strong overlapping regime of Fano resonance, the collision and merging of resonance zeros take place and these zeros move off from the real axis of energy in complex conjugate pairs. The periodic motion of both transmission zeros and resonance poles as a function of a magnetic field is discussed.

DOI: [10.1103/PhysRevB.72.115310](https://doi.org/10.1103/PhysRevB.72.115310)

PACS number(s): 73.21.La, 73.23.Ad, 73.63.Kv, 85.35.Ds

Transmission resonances in multibarrier resonant-tunneling structures have been extensively studied, using Breit-Wigner (BW) expressions in the description of resonant tunneling effects. It is well known that resonant-transmission phenomena are related to the quasibound states of the systems. According to the BW formalism, the scattering amplitude of the transmission possesses a pole for each quasibound state in the complex-energy plane. The real part of a pole can be interpreted as the energy of a quasibound state, and the imaginary part can be connected with the lifetime of this state.¹ When more than one resonant quasibound state is present in a one-channel system, for instance, in a three-barrier system, the resonance levels interact each other and result in the overlapping of resonances.^{2,3} In this situation, therefore, the single BW formula is no longer valid due to the overlapping of resonances. Hence, the interference effects of resonances have been studied by examining the formation of double poles in the transmission amplitude and the effect on the collision of two poles (or merging of two resonances) associated with the quasibound states.^{4–6}

In contrast to multibarrier resonant-tunneling structures, quantum nanostructures such as Aharonov-Bohm (AB) rings and two-dimensional (2D) electronic waveguides, where alternative electronic paths may be realized, possess both transmission zeros and resonance poles. This characteristic of a zero-pole pair, called Fano resonance,⁷ has been particularly predicted and observed in a hybrid system of an AB ring and a quantum dot (QD) both theoretically and experimentally.^{8–21} This Fano effect arises from quantum mechanical interference between the discrete state of the QD in one arm and the continuum in the other arm. The profile of the Fano asymmetric lineshape in the transmission depends on the strength of the coupling between discrete and continuum states, and on the phase difference between the paths. Here, the scattering amplitude near the zero-pole pair behaves like a dipole, where the pole plays the role of a particle and the zero plays the role of a hole (antiparticle).^{22–27} Furthermore, the collapse of the particle and hole has been stud-

ied in a quasi-one-dimensional constriction with an attractive and finite-size impurity by modulating the parameters of the system.^{26,27}

In this article we investigate the interaction of Fano resonances in the transmission for an AB ring with coupled double QDs. When the overlapping of two Fano resonances takes place in the transmission, two Fano dipoles in the complex-energy plane form a quasiparticle, which behaves as a coupled object—a “*Fano quadrupole*.” In the regime of strong overlapping resonances, which can be tuned by the interaction parameter between two QDs, the collision of transmission zeros occurs, and these zeros leave the real-energy axis and move away in opposite directions in the complex-energy plane. We also obtain an analytical expression of the transmission zeros, and show that these zeros are generally complex when two quasibound states lie close together in energy. Finally, we show a periodic motion of the resonance pole and transmission zero in the complex-energy plane as a magnetic field through the AB ring is changed.

The model we study is an AB ring, where a coupled double QD is embedded in one of its arms, as schematically shown in Fig. 1. Here, double QDs can be formed by three electrodes that play a role of the barriers for electrons in the lower arm, and the coupling between two QDs is controlled by the middle electrode. We consider both arms of the ring and the leads as perfect waveguides and adopt a single-propagating channel in the quasi-one-dimensional approximation. Propagating waves in the leads and perfect regions of the arms are assumed to be in the form $\psi(x, y) \propto e^{\pm ikx} \varphi(y)$, where x is the local coordinate along the waveguide, y is the transverse coordinate [transverse wave function is $\varphi(y)$], and wave vector $k = \sqrt{2mE}/\hbar$ of an electron with energy E in the open channel.

In order to connect incoming and outgoing waves at the junctions of the ring and the leads, we employ a simple junction model,²⁸ where a scattering matrix describes the splitting of the electron wave functions at the junction. Using the amplitudes of electron waves in the ring where the relevant

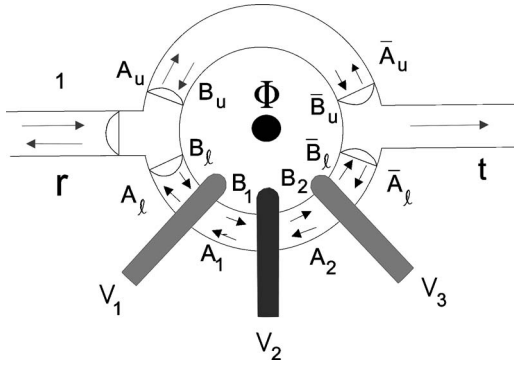


FIG. 1. Geometry of the AB ring with coupled QDs. Three electrodes in the lower arm produce the depletion regions in the two-dimensional electron gas and play the role of the barriers for electrons with potentials V_1 , V_2 , and V_3 . The interaction between two QDs is controlled by the middle electrode marked by a black color.

parameters are defined in Fig. 1, the electron transmission from left to right leads through both the upper and lower arms can be expressed by

$$\begin{pmatrix} \bar{A}_u \\ \bar{B}_u \end{pmatrix} = e^{-i\theta/2} M_u \begin{pmatrix} A_u \\ B_u \end{pmatrix}, \quad \begin{pmatrix} \bar{A}_l \\ \bar{B}_l \end{pmatrix} = e^{i\theta/2} M_l \begin{pmatrix} A_l \\ B_l \end{pmatrix}. \quad (1)$$

Here, $\theta = 2\pi\Phi/\Phi_0$ describes the phase shift introduced by the magnetic flux Φ threading the AB ring ($\Phi_0 = h/e$ is the elementary flux quantum), and M_u and M_l are the transfer matrices through the upper and lower arms, respectively. In order to find the transfer matrix M_l in the lower arm, we consider the coupled QDs that are formed by three short-range potential barriers (V_j , $j=1, 2, 3$). Then, the transfer matrix of each barrier has the form

$$M_j = \begin{pmatrix} 1 - iu_j & -iu_j \\ iu_j & 1 + iu_j \end{pmatrix}, \quad (2)$$

where $u_j = mV_j/k$ with $j=1, 2, 3$. The dimensionless matrix element of the potential u_j describes the strength of the repulsive potential barrier. Therefore, the transfer matrix M_l for the lower arm with two QDs can be expressed by

$$M_l = X(L_1 - L_3) M_3 X(L_3 - L_2) M_2 X(L_2 - L_1) M_1 X(L_1), \quad (3)$$

where $X(x) = \text{diag}(e^{ikx}, e^{-ikx})$, L_l is the upper arm length, and the L_1 , L_2 , and L_3 are distances from the left junction to the first, second, and third electrodes, respectively. On the other hand, the transfer matrix M_u for the upper (reference) arm has a simple form as $M_u = X(L_u)$, where L_u is the length of the upper arm.

Using the transfer matrix and the junction matrices,²⁸ we can write connections between the amplitudes:

$$t = \sqrt{\varepsilon} (\bar{A}_u + \bar{A}_l), \quad (4)$$

$$A_u = \sqrt{\varepsilon} + aB_u + bB_l, \quad \bar{B}_u = a\bar{A}_u + b\bar{A}_l,$$

$$A_l = \sqrt{\varepsilon} + bB_u + aB_l, \quad \bar{B}_l = b\bar{A}_u + a\bar{A}_l. \quad (5)$$

Here, ε plays the role of a coupling parameter between the leads and ring, and the coefficients a and b are expressed as a function of ε : $a = \frac{1}{2}(\sqrt{1-2\varepsilon} + 1)$ and $b = \frac{1}{2}(\sqrt{1-2\varepsilon} - 1)$. After some matrix manipulations, we obtain the full transmission amplitude $t(E, \Phi)$ analytically as

$$t(E, \Phi) = \frac{i\varepsilon e^{i\theta} N(E, \Phi)}{D(E, \Phi)}. \quad (6)$$

Here, the numerator of Eq. (6) can be written as

$$N(E, \Phi) = e^{i[\gamma+2(\delta+\eta)]} [N_0(E, \Phi) + \xi N_1(E, \Phi)], \quad (7)$$

where

$$N_0(E, \Phi) = 4i[\sin \gamma + e^{i\theta/2}\{4u \sin \delta[\cos 2\eta \sin \delta + (\cos \delta + u \sin \delta)\sin 2\eta] + \sin 2(\delta + \eta)\}],$$

and

$$N_1(E, \Phi) = 8iu e^{i\theta/2} [\cos \eta \sin \delta + (\cos \delta + 2u \sin \delta)\sin \eta],$$

with $u \equiv u_1 = u_3$, $\delta = kL_1$, $\eta = k(L_2 - L_1)$, $\gamma = kL_u$, and the interaction parameter between two QDs is $\xi (\equiv u_2/u_1 = V_2/V_1)$. On the other hand, the denominator of Eq. (6) can be expressed by

$$D(E, \Phi) = D_0(E, \Phi) + \xi D_1(E, \Phi), \quad (8)$$

where

$$D_0(E, \Phi) = e^{i(\gamma+2(\delta+\eta))} (1 + e^{i\theta}) + e^{i\theta/2} u^2 (e^{4i\delta} + 4e^{4i\eta} + e^{2i(\gamma+2\eta)}) - 4e^{2i\delta} u(u-i) + 4(u-i)^2 - e^{i\theta/2} [e^{2i\gamma}(u-i)^2 + 4e^{2i(\delta+2\eta)} u(u+i) - e^{4i(\delta+\eta)}(u+i)^2],$$

and

$$D_1(E, \Phi) = ie^{i(\theta/2+2\gamma)} u^3 (e^{2i\eta} - 1)^2 - ie^{i(\theta/2-2(\delta+\eta))} \times \{\sin \delta [3i \cos \eta + \sin \eta (1 + 6iu) - \cos \delta (\cos \eta + (2u - i3)\sin \eta)^2]\}. \quad (9)$$

From Eqs. (7) and (8), we can determine the positions of transmission zeros and resonance poles by setting $N(E, \Phi) = 0$ and $D(E, \Phi) = 0$. We solve these two transcendental equations numerically by using standard routines. In addition, the total transmission probability through the ring as a function of the electron energy and a magnetic flux is given by $T = |t(E, \Phi)|^2$ and the conductance is defined by $G = (2e^2/h)T$ according to the Landauer-Büttiker formalism.

In our calculations, we present results for the following parameters of the ring and dots: the effective electron mass is $m = 0.067m_0$ for GaAs and the geometrical parameters of the ring and positions of gates are chosen to be $L_u = L_l = 80$ nm, $L_1 = 10$ nm, $L_2 = 40$ nm, and $L_3 = 70$ nm. The scattering parameters describing two coupled QDs in the lower arm are used for $a_s V_j = 0.2$ eV nm ($j=1, 3$), where the width and heights of the barriers are set to $a_s = 4$ nm and $V_1 = V_3 = 50$ meV, respectively. The interaction between two QDs, which leads to the overlapping of resonances due to the coupling between the quasibound states, can be controlled by the

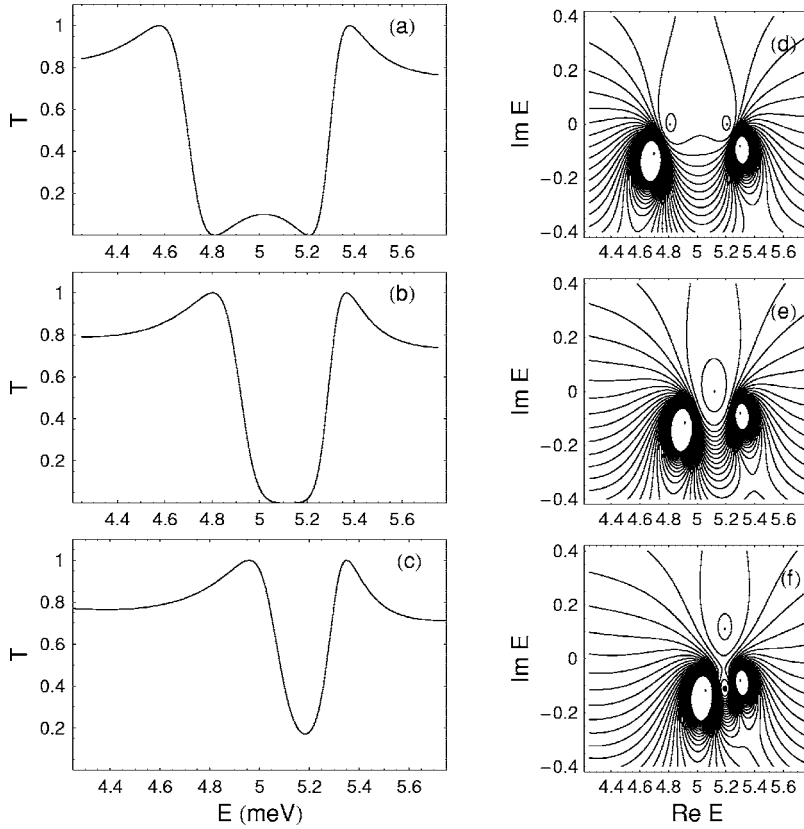


FIG. 2. The total transmission of a nanoscale AB ring as a function of electron energy (the left column) and contour plots of the transmission in the complex-energy plane (the right column) with an increase of the interaction parameter ξ . The two distinct Fano resonances are shown in (a) and (d) for the weak overlapping regime ($\xi=2.5$). Here, there are two poles [$E_b^R=(4.70-i0.11)$ meV and $E_a^R=(5.30-i0.08)$ meV] and corresponding zeros [$E_b^0=4.81$ meV and $E_a^0=5.21$ meV] that both zeros are placed on the real axis of energy. When $\xi=\xi_c=3.77$, the collision of Fano resonances and merging of transmission zeros appear in (b) and (e) with the same zero position as $E_b^0=E_a^0=5.12$ meV. In the strong overlapping regime of Fano resonances ($\xi=5.5$), two transmission zeros [$E_{\pm}^0\approx(5.19\pm i0.11)$ meV] move away in opposite directions from the real-energy axis in (c) and (f).

interaction parameter ξ . A maximum coupling between the ring and the leads is used for $\varepsilon=\frac{1}{2}$ so that the coefficients of Eq. (5) become $a=-b=\frac{1}{2}$.

First, we study the interaction of Fano resonances in the transmission through the AB ring in the absence of a magnetic field by investigating the behavior of transmission amplitude for energy near zero-pole pairs. We consider two quasibound states in the double QDs, where even and odd quasibound states have the energies E_b and E_a , respectively. In Fig. 2, we show both overlapping of the Fano resonances in the transmission as a function of electron energy and a contour plot of transmission in the complex-energy plane for different values of the interaction parameter ξ . In the weak coupling between two QDs, $\xi=2.5$, two distinct Fano resonances in the transmission appear in Fig. 2(a) due to the quantum interference between the continuum states in the upper arm and two discrete states from the coupled QDs in the lower arm. Notice that the width Γ_a of Fano resonance through the odd quasibound state at $E\approx 5.3$ meV is less than the width Γ_b of Fano resonance through the even quasibound state at $E\approx 4.7$ meV ($\Gamma_a<\Gamma_b$). The two transmission zeros (E_a^0 and E_b^0) and two resonance poles ($\tilde{E}_a^R=E_a-i\Gamma_a$ and $\tilde{E}_b^R=E_b-i\Gamma_b$) in the complex-energy plane are seen in Fig. 2(d), where two zeros are separate on the real-energy axis. As ξ becomes a critical value $\xi_c=3.77$, the two Fano resonances in the transmission merge [Fig. 2(b)] and the transmission zeros move toward each other and collide on the real-energy axis [Fig. 2(e)]. When $\xi=5.5>\xi_c$, a minimum of Fano resonance in the transmission does not reach to zero [Fig. 2(c)] and transmission zeros leave the real-energy axis and move away in opposite directions in the complex-energy plane [Fig. 2(f)].

In order to see the behavior of transmission zeros and resonance poles in detail, we calculate the trajectories of the zeros and poles with the explicit expressions from Eqs. (7) and (8) and present in Fig. 3 the trajectories of zeros and poles in the complex-energy plane for a variation of the interaction parameter ξ . As ξ increases, one of Fano resonance

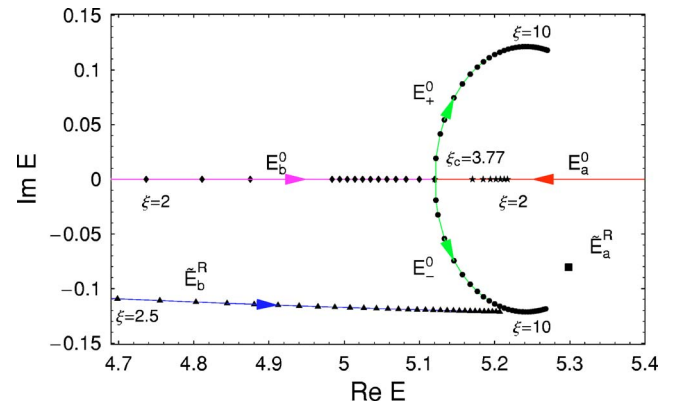


FIG. 3. (Color online) The trajectories of resonance poles ($\tilde{E}_a^R, \tilde{E}_b^R$) and transmission zeros (E_a^0, E_b^0) in the complex-energy plane with an increase of the coupling parameter ξ ($2<\xi<10$). When ξ increases, two zeros E_a^0 (red arrow) and E_b^0 (pink arrow) move toward each other and the collision and merging take place at $\xi_c=3.77$. After merging, two zeros move away from the real-energy axis in opposite directions as complex conjugate pairs (denoted by E_+^0 and E_-^0 with green arrows). The resonance pole \tilde{E}_b^R associated with an even quasibound state moves to the higher energy (blue arrow), and \tilde{E}_a^R arising from the odd quasibound state is nearly motionless [$\tilde{E}_a^R\approx(5.30-i0.08)$ meV].

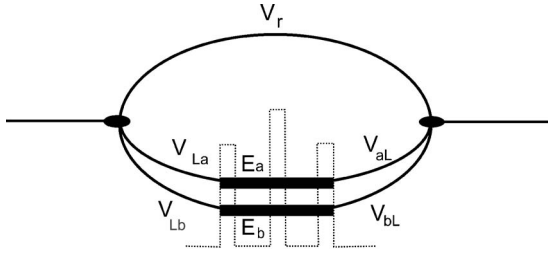


FIG. 4. A schematic diagram for even and odd quasibound states with energies E_b and E_a , connecting with the junction states of the ring by the appropriate matrix elements V_{Lb} , V_{bL} , V_{aL} , and V_{La} . The matrix element of the junctions through the upper arm is denoted by V_r .

zeros E_b^0 (shown as diamonds) arising from even quasibound state in the QDs moves to the higher energy and another zero E_a^0 (shown as stars) arising from odd quasibound state in the QDs moves to the lower energy. When $\xi = \xi_c$, the collision and merging of E_b^0 and E_a^0 takes place at $E_a^0 = E_b^0 = 5.12$ meV. In the strong overlapping regime of Fano resonances ($\xi > \xi_c$), the transmission zeros, denoted by E_+^0 and E_-^0 (shown as circles), move away from the real-energy axis in opposite directions as complex conjugate pairs.

It is interesting to note that the behavior of the resonance poles (\tilde{E}_b^R and \tilde{E}_a^R) is different from that of transmission zeros (E_b^0 and E_a^0). The resonance pole \tilde{E}_b^R arising from an even quasibound state in the QDs is shifted to the higher energy as ξ increases. However, the movement of \tilde{E}_b^R to the higher energy is hindered by one of the transmission zeros E_-^0 at $E \approx 5.24$ meV, which prevents the collision of the resonance poles \tilde{E}_b^R and \tilde{E}_a^R . On the other hand, the resonance pole \tilde{E}_a^R arising from the odd quasibound state in the QDs is nearly motionless because the odd quasibound state of the double QDs is weakly affected by ξ due to short-range potentials in the lower arm of the ring.

In order for zeros of transmission amplitude to confirm to move away from the real axis in the case of overlapping Fano resonances, we calculate the transmission zeros analytically by employing a simple model shown in Fig. 4. We consider two nearest quasibound states in the dots that are even and odd levels with energies E_b and E_a , respectively. These two orthogonal states of the dots in the lower arm can be connected with the junction states of the ring by the appropriate matrix elements V_{Lb} , V_{bL} , V_{aL} , and V_{La} . On the other hand, V_r is defined as the matrix element of the junctions through the reference arm. Notice that these matrix elements are generally complex numbers, and they are dependent on the phase difference between localized wave functions in the dots and propagating waves in the leads. If the energy of an incoming electron from the lead is near the resonant energies of the dots, then the matrix elements that couple an even (odd) quasibound state to the left and right of the dots are real and have same (opposite) signs: $V_{Lb} > 0$ and $V_{bL} > 0$ ($V_{La} > 0$ and $V_{aL} < 0$). With these matrices, we can obtain an exact expression for the scattering amplitude, which has the same structure of Fano zero-pole pairs, as expressed in Eq. (6). Here, the numerator of the scattering amplitude has the form

$$N(E) = (E - E_b)(E - E_a) - (E - E_b)U_{aa} - (E - E_a)U_{bb}, \quad (10)$$

where

$$U_{aa} = \frac{V_{aL}V_{La}}{V_r} \quad \text{and} \quad U_{bb} = \frac{V_{bL}V_{Lb}}{V_r}.$$

Then, the transmission zeros (E_b^0 and E_a^0) can be exactly obtained from the equation $N(E) = 0$, which gives

$$E_{a,b}^0 = \frac{1}{2}(E_a + E_b + U_{aa} + U_{bb} \pm \sqrt{(E_a - E_b + U_{aa} - U_{bb})^2 + 4U_{aa}U_{bb}}). \quad (11)$$

The examination of Eq. (11) indicates that E_b^0 and E_a^0 are off from the real axis of energy when

$$E_a - E_b < U_{bb} + |U_{aa}| + 2\sqrt{|U_{aa}|U_{bb}}, \quad (12)$$

where $U_{bb} > 0$ and $U_{aa} < 0$. This implies that when even and odd quasibound states lie close together in energy, the transmission zeros move off from the real axis of energy. Using the location of these zeros and poles that are generally complex numbers, the transmission amplitude of Eq. (6) near the resonances in Fano overlapping regime can be expressed as

$$t_F(E) \propto \frac{(E - E_a^0)(E - E_b^0)}{(E - E_b + i\Gamma_b)(E - E_a + i\Gamma_a)}, \quad (13)$$

which characterizes the transmission line shape in the vicinity of the transmission zeros and resonance poles.

Since the coupled Fano resonances in the transmission can be tuned by the magnetic flux Φ threading the AB ring, we study a magnetic field dependence of transmission zeros and resonance poles in a strong Fano overlapping regime. The trajectories of zeros and poles in the complex-energy plane as a function of magnetic flux are shown in Fig. 5 for a given interaction parameter $\xi = 5.5$. As Φ increases, the two zeros at $E_+^0 = (5.19 + i0.11)$ meV and $E_-^0 = (5.19 - i0.11)$ meV for $\Phi = 0$ start to move to the higher (green arrow with circles) and lower (red arrow with stars) energies, respectively, until they reach to the real axis. When $\Phi = \frac{1}{2}\Phi_0$, these complex conjugate pairs become real numbers ($E_+^0 = 5.45$ meV and $E_-^0 = 4.95$ meV), which indicates a full reflection of the transmission. When $\frac{1}{2}\Phi_0 < \Phi < \Phi_0$, these zeros continue to move on the other half of the trajectories to complete a stadiumlike orbit. Then, the zero E_+^0 comes to initial position of E_-^0 and *vice versa* for $\Phi = \Phi_0$. In other words, the upper zero E_+^0 circumscribes half of the orbit and then the lower zero E_-^0 replaces the same part of the orbit after the flux is changed by a period. On the other hand, the behavior of the resonance poles is quite different. As Φ increases, each pole at $E_b^R = (5.06 - i0.12)$ meV (shown as triangles) and $E_a^R = (5.30 - i0.08)$ meV (shown as diamonds) for $\Phi = 0$ moves a short nearly straight line periodically. (If $\Phi = \frac{1}{2}\Phi_0$, these two poles are located at the opposite end of the starting points along these lines.)

It is worthwhile noting here that the transmission through

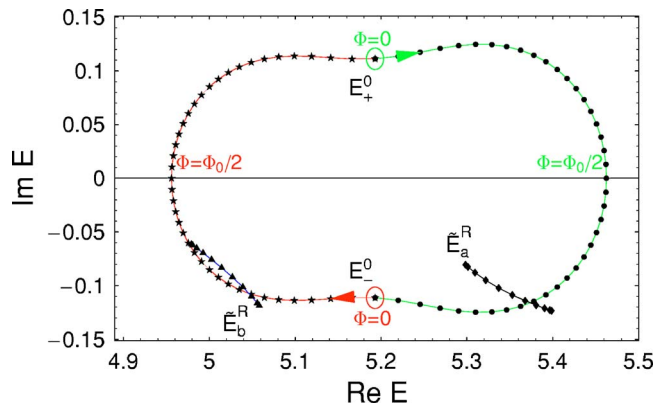


FIG. 5. (Color online) The trajectories of zeros and poles as a function of a magnetic flux for a fixed interaction parameter $\xi = 5.5$. The two zeros for $\Phi=0$ at $E_+^0 = (5.19 + i0.11)$ meV and $E_-^0 = (5.19 - i0.11)$ meV start to move to the right (green arrow) and left (red arrow), respectively, and they reach to the real axis for $\Phi = \frac{1}{2}\Phi_0$ that is a full reflection of the transmission. These zeros continue to move on the other half of the trajectories and complete a stadiumlike orbit for $\frac{1}{2}\Phi_0 < \Phi < \Phi_0$. The resonance poles at $E_b^R = (5.06 - i0.12)$ meV and $E_a^R = (5.30 - i0.08)$ meV for $\Phi=0$ move in a short nearly straight line periodically.

the ring is a periodical function of magnetic flux, which changes the interference between the parts of the wave function in the arms. Hence, the transmission zeros are more sensitive to the magnetic flux because they are defined by wave interference. However, the resonance poles are defined by quasibound energy and move slowly in a magnetic field.

Finally, we present an analytical expression for zero trajectories in the presence of magnetic field using the same model shown in Fig. 4. If a magnetic flux is applied to the loop in the perpendicular direction, each wave function gives a phase shift on the links. The phase shift on the links connecting the dots with the leads is $\theta/4$ so that the matrix elements between the dots and the leads are replaced by $V_{n,m} \rightarrow V_{n,m} e^{\pm i\theta/4}$, where the sign depends on the propagation direction of an electron. On the other hand, the phase shift through the reference arm is $\theta/2$, and so we can set $V_r \rightarrow V_r e^{-i\theta/2}$. Then, the effective matrix elements can be written as $U_{aa} \rightarrow U_{aa} e^{i\theta}$ and $U_{bb} \rightarrow U_{bb} e^{i\theta}$, and the analytical ex-

pression for the transmission zeros in the presence of magnetic field is

$$E_{a,b}^0 = \frac{1}{2}(E_a + E_b + (U_{aa} + U_{bb})e^{i\theta} \pm \sqrt{[E_a - E_b + (U_{aa} - U_{bb})e^{i\theta}]^2 + 4U_{aa}U_{bb}e^{i2\theta}}). \quad (14)$$

This expression indicates the periodic trajectories for transmission zeros as Φ changes, which is shown in Fig. 5. We note that for the nonoverlapping regime when Fano dipoles exist, the zeros move in separate circular orbits near their associated poles (not shown here). In the strong overlapping regime, however, the zeros as a coupled object move in a common stadiumlike orbit around two coupled poles. This means that two overlapped Fano resonances can be considered as a combined object called the “*Fano quadrupole*.”

In summary, the Fano interference effects have been investigated in an AB ring with two coupled QDs in the presence of magnetic field. In this system, we have examined new effects on the collision of Fano dipoles and its manifestation in the transmission. It was shown that the proximity of the Fano dipoles leads to the shift of zero resonances in the complex-energy plane. The scattering amplitude near a Fano zero-pole pair behaves like the amplitude of a dipole when the pole and the zero play the role of a particle and a hole (antiparticle), respectively. In a nonoverlapping regime these dipoles behave as independent objects. We have shown here that in the strong Fano overlapping regime, the trajectories for transmission zeros as a function of a magnetic flux move in a common stadiumlike orbit around two coupled poles and then two Fano dipoles behave as a coupled object—the “*Fano quadrupole*.” Therefore, we can consider this Fano coupled object as two-level systems that have additional parameters for quantum control of device’s conductance.

ACKNOWLEDGMENTS

This work is supported by the Indiana 21st Century Research and Technology Fund, and the National Science Foundation under Grant No. EEC-0228390.

- ¹M. Goldberg and K. Watson, *Collision Theory* (Wiley, New York, 1964).
- ²G. García-Calderón, R. Romo, and A. Rubio, *Phys. Rev. B* **47**, 9572 (1993).
- ³Zhi-an Shao and W. Porod, *Phys. Rev. B* **51**, 1931 (1995).
- ⁴F.-M. Dittes, *Phys. Rep.* **339**, 215 (2000).
- ⁵J. S. Bell and C. J. Goebel, *Phys. Rev.* **138**, B1198 (1965).
- ⁶K. E. Lassila and V. Ruuskanen, *Phys. Rev. Lett.* **17**, 490 (1966).
- ⁷U. Fano, *Phys. Rev.* **124**, 1866 (1961).
- ⁸A. Yacoby, R. Schuster, and M. Heiblum, *Phys. Rev. B* **53**, 9583 (1996).
- ⁹P. S. Deo and A. M. Jayannavar, *Mod. Phys. Lett. B* **10**, 787 (1996).

- ¹⁰R. Schuster, E. Buks, M. Heiblum, D. Mahalu, V. Umansky, and H. Shtrikman, *Nature (London)* **385**, 417 (1997).
- ¹¹C. M. Ryu and S. Y. Cho, *Phys. Rev. B* **58**, 3572 (1998).
- ¹²K. Kang, *Phys. Rev. B* **59**, 4608 (1999).
- ¹³J. Göres, D. Goldhaber-Gordon, S. Heemeyer, M. A. Kastner, H. Shtrikman, D. Mahalu, and U. Meirav, *Phys. Rev. B* **62**, 2188 (2000).
- ¹⁴W. Hofstetter, J. König, and H. Schoeller, *Phys. Rev. Lett.* **87**, 156803 (2001).
- ¹⁵A. A. Clerk, X. Waintal, and P. W. Brouwer, *Phys. Rev. Lett.* **86**, 4636 (2001).
- ¹⁶K. Kobayashi, H. Aikawa, S. Katsumoto, and Y. Iye, *Phys. Rev. Lett.* **88**, 256806 (2002).

- ¹⁷O. Entin-Wohlman, A. Aharony, Y. Imry, Y. Levinson, and A. Schiller, *Phys. Rev. Lett.* **88**, 166801 (2002).
- ¹⁸T. S. Kim, S. Y. Cho, C. K. Kim, and C. M. Ryu, *Phys. Rev. B* **65**, 245307 (2002).
- ¹⁹A. Aharony, O. Entin-Wohlman, and Y. Imry, *Phys. Rev. Lett.* **90**, 156802 (2003).
- ²⁰T. S. Kim and S. Hershfield, *Phys. Rev. B* **67**, 235330 (2003).
- ²¹K. Kobayashi, H. Aikawa, A. Sano, S. Katsumoto, and Y. Iye, *Phys. Rev. B* **70**, 035319 (2004).
- ²²E. Tekman and P. F. Bagwell, *Phys. Rev. B* **48**, 2553 (1993).
- ²³Zhi-an Shao, W. Porod, and C. S. Lent, *Phys. Rev. B* **49**, 7453 (1994).
- ²⁴J. U. Nöckel and A. D. Stone, *Phys. Rev. B* **50**, 17 415 (1994).
- ²⁵R. C. Bowen, W. R. Frensley, G. Klimeck, and R. K. Lake, *Phys. Rev. B* **52**, 2754 (1995).
- ²⁶C. S. Kim, A. M. Satanin, Y. S. Joe, and R. M. Cosby, *Phys. Rev. B* **60**, 10962 (1999).
- ²⁷C. S. Kim, O. N. Roznova, A. M. Satanin, and V. B. Shtenberg, *JETP* **94**, 992 (2002).
- ²⁸S. Datta, *Electronic Transport in Mesoscopic Systems* (Cambridge University Press, Cambridge, 1995).